

High-temperature properties of fermionic alkaline-earth-metal atoms in optical lattices

Kaden R. A. Hazzard,^{1,2,3,*} Victor Gurarie,² Michael Hermele,² and Ana Maria Rey^{1,2,3}

¹JILA, University of Colorado, Boulder, Colorado 80309-0440, USA

²Department of Physics, University of Colorado, Boulder, Colorado 80309-0440, USA

³NIST, Boulder, Colorado 80309-0440, USA

(Received 30 October 2010; revised manuscript received 17 February 2012; published 26 April 2012)

We calculate experimentally relevant properties of trapped fermionic alkaline-earth-metal atoms in an optical lattice, modeled by the $SU(N)$ Hubbard model. We employ a high-temperature expansion that is accurate when the temperature is larger than the tunneling rate, similar to current regimes in ultracold atom experiments. In addition to exploring the Mott insulator-metal crossover, we calculate final temperatures achieved by the standard experimental protocol of adiabatically ramping from a noninteracting gas, as a function of initial gas temperature. Of particular experimental interest, we find that increasing N for fixed particle numbers and initial temperatures gives substantially *colder* Mott insulators after the adiabatic ramping, up to more than a factor of 5 for relevant parameters. This cooling happens for all N , fixing the initial entropy, or for all $N \lesssim 20$ (the exact value depends on dimensionality), at fixed, experimentally relevant initial temperatures.

DOI: 10.1103/PhysRevA.85.041604

PACS number(s): 67.85.-d, 03.75.Ss, 37.10.Jk, 75.10.Jm

Introduction. The recent achievement of Fermi degeneracy and Bose-Einstein condensation in ultracold alkaline-earth-metal atoms [1] opens great opportunities in quantum information processing [2], quantum simulations [3], atomic clock experiments [4], and other precision measurements [5]. One fundamental property of fermionic alkaline-earth-metal atoms is their intrinsic $SU(N = 2I + 1)$ symmetry in the nuclear spin (I) degrees of freedom (bosonic alkaline-earth-metal isotopes in contrast have even-even nuclei and necessarily $I = 0$ [6]). Fermionic alkaline-earth-metal atoms loaded in an optical lattice, as recently experimentally realized in Ref. [7], are described by the $SU(N)$ Hubbard model where N can be varied for a single isotope from 2 to $2I + 1 \leq 10$ by selectively populating hyperfine levels. Cold atom realizations of this model open up a range of exciting and exotic physics relevant to condensed matter: It is a simple limit of multiorbital models describing transition-metal oxides, is important in theoretical generalizations of the Fermi-Hubbard model, and displays phenomena such as possible antiferromagnetism, superconductivity, nematic order, valence bond, and spin-liquid phases [3,8–11].

As a first step toward reaching the low temperatures necessary to observe these states, here we study the $SU(N)$ Hubbard model's finite-temperature Mott-metal crossover. One particularly interesting finding is that increasing N while fixing the initial temperature can lead to a more than fivefold decrease, compared to $N = 2$, in final temperature after adiabatic lattice loading, relative to the temperature scales of interesting physics.

We calculate density and entropy profiles of lattice alkaline-earth-metal atoms to second order in t/T , the tunneling rate over the temperature [see Eq. (1)]. This calculation is accurate for $T \gg t$, regardless of the on-site interaction U . This includes the “unquenched Mott insulator (MI)” regime $t \ll T \ll U$ that has been realized in $SU(2)$ alkali gases [12]. For the $SU(2)$ spin-1/2 case, sophisticated, numerically

intensive algorithms have yielded series to tenth order [13]. For properties in the experimental regime, $T \gtrsim t$ in three dimensions, the second-order expansion agrees quantitatively ($\lesssim 1\%$ error) with longer series and dynamical mean-field theory [14]. We also calculate final temperatures achieved by standard experimental adiabatic ramping protocols.

Excitingly, our calculations show that applying the same protocols as in $SU(2)$ experiments will generate colder, less compressible MI states as N increases, up to $N \sim 20$. An entropic argument supplementing the high-temperature expansion supports that this effect persists down to temperatures on the order of the superexchange energy where interesting magnetic physics appears.

Alkaline-earth-metal atoms in deep optical lattices are well described by the $SU(N)$ Fermi-Hubbard model [3]

$$H = -t \sum_{(ij),\alpha} f_{\alpha,i}^\dagger f_{\alpha,j} + \frac{U}{2} \sum_i \hat{n}_i (\hat{n}_i - 1) + \sum_i V_i n_i, \quad (1)$$

where $f_{\alpha,j}$ is a fermionic annihilation operator destroying a particle of flavor α at site j , satisfying anticommutation relations $\{f_{\alpha,i}, f_{\alpha',j}^\dagger\} = \delta_{\alpha,\alpha'} \delta_{i,j}$, $\sum_{(ij)}$ indicates a sum over nearest neighbors, V_i is the trapping potential at site i , α and α' are flavor indices that run from 1 to N , and the total on-site density is $\hat{n}_i \equiv \sum_{\alpha} f_{\alpha,i}^\dagger f_{\alpha,i}$.

Atomic limit: Experimental observables and $T/U \ll 1$ and $T/U \gg 1$ limits. First we give results in the atomic limit ($t = 0$), the zeroth-order term in the high-temperature series expansion in t/T . Throughout, we present analytic results for the free-energy density \mathcal{F} , from which the other observables considered can be obtained by differentiating: The average filling and entropy per site are $\langle n \rangle = -\partial \mathcal{F} / \partial \mu$ and $s = -\partial \mathcal{F} / \partial T$.

For the homogeneous system, the grand canonical free energy per site for $t = 0$ is [8] $\mathcal{F}_0 = -T \ln z_0$ with the on-site partition function $z_0 = \sum_{n=0}^N C_n^N e^{-\beta \epsilon_0(n)}$, where $\epsilon_0(n) \equiv (U/2)n(n-1) - \mu n$, $\beta \equiv 1/T$, $k_B = \hbar = 1$ throughout, and C_n^N is the binomial coefficient. The average filling is $n_0 = \langle n \rangle_0$ where $\langle O \rangle_0$ of a one-site operator O is defined as

*kaden.hazzard@colorado.edu

$\langle O \rangle_0 \equiv \frac{1}{z_0} \sum_n O(n) C_n^N e^{-\beta \epsilon_0(n)}$. The entropy is $s_0 = \ln z_0 + (1/T) \langle \epsilon_0(n) \rangle_0$.

It is illuminating to consider the observables in the $T \ll U$ and $T \gg U$ limits. In the $T \gg \{U, \mu\}$ limit the on-site partition function is $z_0(T \gg U) \approx \sum_{n=0}^N C_n^N = 2^N$, the density is $n_0(T \gg U) \approx N/2$, and the entropy density is $s_0(T \gg U) \approx N \ln 2$. In contrast, in the MI limit defined by $t \ll T \ll U$ and $\mu \neq Un$ for all n , one term dominates z_0 so that $z_0 \approx C_{n_0}^N e^{-\beta \epsilon_0(n_0)}$, with n_0 chosen to minimize $\epsilon_0(n_0)$, and $s_0 \approx \ln(C_{n_0}^N)$. The metal boundary separating the n' and $n' + 1$ MI's has similarly simple expressions.

Cold atomic systems are trapped in trapping potentials, which we treat with a Thomas-Fermi or local density approximation (LDA) [15]. We take the trapped system's properties at a point in space \mathbf{r} to be those of the homogenous system at a chemical potential $\mu(\mathbf{r}) = \mu_0 - V(\mathbf{r})$. This is accurate when V varies slowly compared to the state's characteristic lengths, which is frequently well satisfied. For simplicity, and as an accurate description of most traps, we approximate $V(\mathbf{r}) = m\omega^2 r^2/2$, where m is the particle mass and ω is the trap frequency.

Figure 1 shows the density n and entropy s profiles, illustrating the Mott plateaus at low temperatures. It also

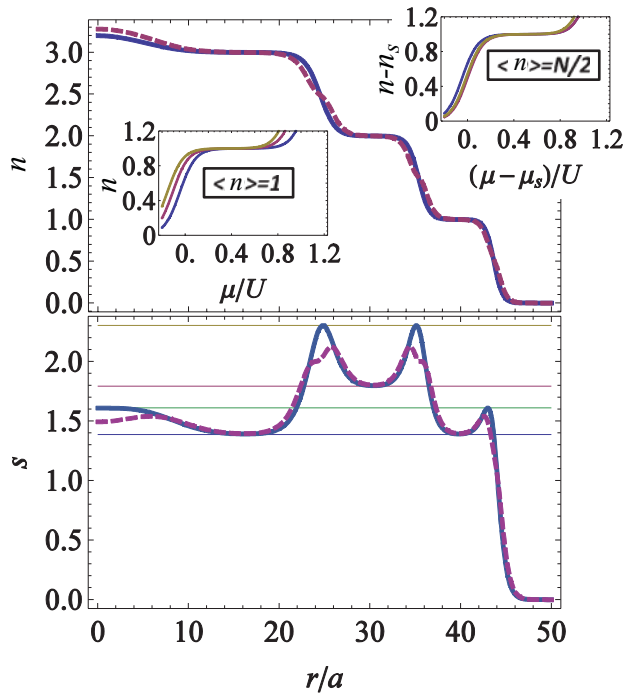


FIG. 1. (Color online) Observables as a function of distance to trap center r for $N = 4$ at $T/U = 1/15$, $\mu/U = 3.0$, and in three dimensions. Top: Density (solid: atomic limit; dashed: $t/U = 0.04$). Although the value of the t/T is not deep in the regime where the high-temperature expansion is valid, such a large value was chosen so the effects would be visible in the density profile. Insets: Density vs μ for $N = 2, 5$, and 10 , showing N and n dependence. Left inset: Zoom around the $n = 1$ shell. Right inset: Zoom around $n = 1, 3, 5$ for $N = 2, 5, 10$ with density and μ shifted by $n_s = 0, 2, 4$ and $\mu_s = 0, 2, 4$ so that the Mott shells nearly overlap on the plot. Bottom: Entropy (solid: atomic limit; dashed: $t/U = 0.016$; thin horizontal: $T \ll U$ deep Mott and deep metal limits discussed in text).

shows the effects of tunneling calculated later. At temperatures $T/U \gtrsim 0.2$ all curves are smooth and lack visible Mott plateaus (not shown). Figure 1's insets show the N dependence near $n = 1$ and $n = N/2$. Although the density profiles shown are at temperatures below the regime of validity $t/T \gtrsim 1$, one finds that the theory is inaccurate only near the metal between Mott shells [14]. Working deeper in the approximation's regime of validity would lead to a smaller effect, invisible to the eye. However, the qualitative effects are the same, only smaller.

Adiabatic loading. We theoretically study the protocol used to realize bosonic [16] and fermionic [12,17] MI's, essential to understanding and optimizing the process. Remarkably, we find that for the relevant N , the final T substantially *decreases* with increasing N .

The procedure used to create MI's is to first create a degenerate, weakly interacting gas without a lattice. A lattice is then ramped up to its final value. Ideally, the ramp is sufficiently slow to be adiabatic. The adiabatic limit is approached in recent boson experiments [16,18], and with (presumably much) less than $\sim 50\%$ entropy increases in SU(2) Fermi experiments [12,17]. The limits of adiabaticity are beyond the scope of our present work.

In the adiabatic limit entropy is conserved, and given the initial state's particle number \mathcal{N} and entropy S_i , one can determine the final temperature by matching the particle number and entropy to the initial state. S_i is controlled and measured through the temperature. Thus, we must first determine S_i from the initial temperature T_i .

For any initial state sufficiently cold to reach a MI, the initial gas will be deeply degenerate, $T_i \ll \mu$. For large \mathcal{N} , the harmonic trap can be treated as having a continuous density of states $\nu(\epsilon) = (\epsilon/\omega)^{d-1}/[\omega(d-1)!]\Theta(\epsilon)$, with $\Theta(\epsilon)$ the Heaviside step function. Using this, the total particle number and entropy of a d -dimensional trapped system are $\mathcal{N} = \frac{N}{d!} (\frac{\mu}{\omega})^d$ and $S_i = \frac{T_i}{\omega} \frac{N\pi^2}{3(d-1)!} (\frac{\mu}{\omega})^{d-1}$ to lowest order in T_i/μ . (To the same accuracy, the Fermi temperature is $T_F = \mu$.) At fixed \mathcal{N} , these imply $S_i \propto N^{1/3}$. This will be crucial, and the Supplemental Material [19] derives and explains it.

Figure 2 shows our adiabatic loading results for a three-dimensional system. Although specific values depend on microscopic parameters such as the scattering length a_s , lattice spacing a , and trap length ℓ , our qualitative findings are independent of these. We determine the Hubbard parameters using the standard deep lattice results [20] for experimental parameters consistent with Ref. [21].

Figure 2 shows the final temperature after adiabatic loading on a logarithmic scale as a function of T_i for $N = 2, 4, 6$, using experimentally relevant parameters at fixed final lattice depth. Figure 2 (inset) illustrates the effect of cooling on density profiles obtained by increasing N . For reference, the coldest alkaline-earth-metal gases in the weakly interacting regime (initial state) have roughly $T_i/\mu = 0.14$ for ^{173}Yb ($N = 6$) and $T_i/\mu = 0.26$ [21] for ^{87}Sr ($N = 10$) [1]. Also, we have found that for deep lattices, the final rescaled temperature T/U as a function of T_i/ω is nearly independent of lattice depth V_0 , except for an overall scale factor.

One of our most interesting findings is the final temperature's N dependence: increasing N produces colder MI's when initial parameters are fixed in an experimentally realistic way. In particular, this holds for fixed T_i , as occurs

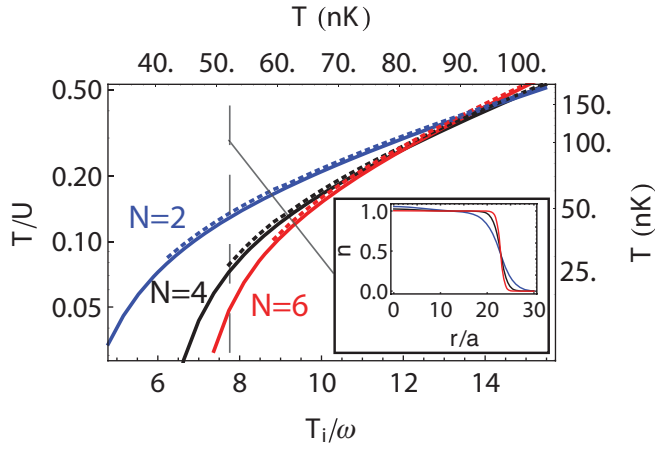


FIG. 2. (Color online) Adiabatic loading: Final temperature T/U on a log scale as a function of initial temperature T_i/ω for $N = 2, 4, 6$ (top to bottom at low temperatures) at lattice depth $V_0 = 18E_R$, in three dimensions for $t/U = 0$ (solid) and $t/U = 0.07$ (dashed) calculated with the second-order high-temperature series. Parameters are fixed to experimental values for ^{173}Yb [21]: We find $U/\omega = 50$, $a/\ell = 0.4$, and $\mathcal{N} = 5 \times 10^4$ particles using standard optical lattice results for U [20]. The experimental initial gas temperature is $T_i/\omega = 5.2$ ($T_i/\mu = 0.14$ for $N = 6$). Parameters are roughly the same for other alkaline-earth-metal atom experiments. Inset: Density profiles after adiabatic loading for $T_i/\omega = 7.3$ ($T_i/\mu = 0.14, 0.17, \text{ and } 0.20$ for $N = 2, 4, 6$, respectively).

when the initial gas is sympathetically cooled by another species—an even more favorable situation is considered below. A corollary follows since $SU(N)$ gases can be produced with T_i 's comparable to current alkali $SU(2)$ lattice experiments: MI's with $T \sim t \ll U$ or even lower are well within reach for $SU(N)$ systems.

Our findings are a direct consequence of the rapidly increasing $t \ll T \ll U$ MI entropy. Considering the $n = 1$ state for simplicity, its entropy grows as $S_f \propto \ln N$, since each of the N flavors is equally likely to occupy a site (the reduced Pauli blocking plays no role in the atomic limit). For the relevant range of N , $N \lesssim 20$, this logarithm grows faster than the initial-state entropy, $S_i \propto N^{1/3}$, given previously. Increasing N , the MI's entropy increased more than does S_i , and therefore the resulting MI is colder as one increases N , as observed in Fig. 2. In the $t \ll T \ll U$ limit of the atomic limit theory for central unit occupation and negligible multiple occupancy, in addition to the LDA approximation used perviously, the calculation yields a simple expression for T_f : $T_f = aN^{2/3}(T_i/\omega) - b \ln N$. This demonstrates the decreasing temperature T_f with increasing N for small T_i/ω . The details and values of a and b are discussed in the Supplemental Material [19]. The situation is even more favorable if one lets n scale with N : One finds that the MI entropy is proportional to N and thus the final states get colder with increasing N for all N . A similar argument explains the reversal of this effect at high temperatures (see the Supplemental Material [19]).

While we observe this dramatic cooling when fixing T_i , the actual situation may be even more favorable. Other cooling procedures may fix S_i , or equivalently T_i/μ , independent of N . An alternative way to think about this is to realize

that the thermodynamic limit is taken fixing $\omega(\mathcal{N}/N)^{1/d}$. Thermodynamic functions are functions of this quantity, and thus S_i is a function of $T/[\omega(\mathcal{N}/N)^{1/d}]$, so that fixing S_i leads to $T_i \propto 1/N^{1/d}$, which decreases with increasing N . Thus, the final temperature decreases even faster than in the fixed T_i case. Since we know how T_i scales with N at fixed S_i , Fig. 2 allows one to read off the final temperatures. For fixed S_i the MI will get colder with increasing N for all N , even for $n = 1$. Evaporative cooling is a candidate to fix S_i , with an added benefit that Pauli blocking becomes less important as N increases so that $S_i \propto T_i/\mu$ may actually decrease.

Returning to the adequacy of our description of the experimental loading process, there are two main issues: nonadiabaticity and external confinement changes due to the lattice laser. Although nonadiabatic effects are difficult to calculate, if one assumes the entropy increases by a factor of F during the lattice ramp, it is simple to read off the final temperature from Fig. 2: A factor of F increase in entropy is equivalent to a factor of F increase in T_i , since $S_i \propto T_i$. We have treated the effects of external confinement changes (not presented) and find that, as expected from our qualitative arguments, this affects the reduction in temperature obtained from increasing N by amounts on the order of a few percent.

Nonzero tunneling. To incorporate tunneling, we perform a second-order expansion in t/T , equivalent to a finite-temperature t/U expansion. Analogous results were recently applied to $SU(2)$ experiments [14], where they are quantitatively accurate ($\lesssim 1\%$ error) when $T \gtrsim t$ for the metallic region (e.g., $n \sim 1.3$) and for much lower T elsewhere (e.g., $n \sim 0, 1, \text{ and } 2$) [22,23]. Ongoing experiments are in this regime, although $SU(2)$ experiments have begun to reach $T \lesssim t$. Longer series maintain agreement for $T \gtrsim t$, but, being divergent, series of all lengths give unphysical results for $T \lesssim t$. Nevertheless, they may be useful to understand low-temperature physics by analyzing their analytic structure [13].

We find the free-energy density to $O[(t/T)^2]$ is $\mathcal{F} = \mathcal{F}_0 - 2Td(\frac{t}{U})^2 \langle n \rangle_r [1 - \frac{\langle nl \rangle_r}{N \langle n \rangle_r}]$, where we define

$$\left\{ \begin{array}{l} \langle n \rangle_r \\ \langle nl \rangle_r \end{array} \right\} = \frac{1}{z_0^2} \left[\frac{1}{2} \left(\frac{U}{T} \right)^2 \sum_n (C_n^N)^2 \left\{ \begin{array}{l} n \\ n^2 \end{array} \right\} e^{-2\beta\epsilon_0(n)} + \sum_{l=0}^N \sum_{\substack{l=0 \\ l \neq n}}^N \left\{ \begin{array}{l} n \\ nl \end{array} \right\} g_{nl} \right], \quad (2)$$

with $g_{nl} \equiv C_n^N C_l^N \left[\frac{e^{-\beta U(n-l+1) + \beta U(n-l+1)-1}}{(n-l+1)^2 e^{\beta\epsilon_0(n) + \epsilon_0(l)}} \right]$. We note the second-order corrections can capture some nearest-neighbor spin-spin correlations, in contrast to the atomic limit.

Figure 1 shows tunneling's consequences. In the density profiles, we see that it reduces the MI's size, as expected. In the entropy profiles, tunneling slightly increases the MI entropy while significantly decreasing the metal entropy: In the MI, tunneling reduces the excitation gap, increasing the entropy, while in the metal, the increasing bandwidth lowers the low-energy density of states, decreasing the entropy. We also observe (Fig. 1 insets) that although the magnitude of the tunneling corrections depends only weakly on n , the N dependence depends more strongly on n . For $n = 1$, there is

noticeable N dependence of the tunneling corrections, while there is little for $n = N/2$.

We finally have considered the effect of tunneling on the adiabatic loading, and find that it increases the final temperature. This may be understood from Fig. 1: Tunneling reduces the total entropy as a consequence of a small increase in MI entropy and a relatively larger decrease in metal entropy. The effects are small when t/T is small, as seen in Fig. 2.

We note that the corrections to LDA, important mainly in the initial weakly interacting gas, are on the order of a few percent. Therefore, these give a small correction to the cooling, comparable to the tunneling corrections for a $V_0 = 10E_R$ lattice.

Magnetic physics near the superexchange temperature. The high-temperature expansion results presented above give a fairly comprehensive picture for temperatures $T \gtrsim t$, an interesting and, for the near future, the most experimentally relevant regime. However, a long-term experimental goal is to reach interesting, possibly exotic, low-temperature magnetic phases. These occur at a much lower temperature scale $T \lesssim J \sim t^2/U$.

To study these lower temperatures, we use arguments distinct from the high-temperature expansion. We note that the $SU(N)$ Heisenberg model associated with the density n MI for $t \ll U$ has, at high temperatures, $s = \ln C_n^N$. Any entropy below this results from superexchange. Hence, the entropy at which superexchange begins to play a role is the same as the entropy in the $T \ll U$ regime found in the zeroth-order high-temperature expansion. Based on this simple argument we expect that the decrease of final temperatures

with increasing N after lattice loading applies down to the scale where superexchange first becomes relevant. Consequently, the T_i required to reach temperatures where magnetic physics becomes relevant is roughly expected to increase with N .

Conclusions and discussion. We studied the metal-Mott insulator crossover using a high-temperature series expansion technique, up to second order in t/T . We calculated the density and entropy in the atomic limit and quantified how tunneling reduces the size of the Mott insulating region, its flavor number (N), and filling (n) dependence, and how it increases the Mott entropy while decreasing the metal entropy.

Additionally, we studied the standard experimental protocol used to realize Mott insulators and showed that the final temperatures significantly decrease with increasing N . We present arguments suggesting this persists down to temperatures where superexchange and interesting magnetic physics manifests.

Three-body losses might limit the observability of the shell structure with $n > 2$. Nevertheless, based on Ref. [24]'s theory we find, at least for ^{87}Sr , that even fillings $n \lesssim 5$ may live sufficiently long to explore their many-body physics.

Acknowledgments. We thank Salvatore Manmana, Adrian Feiguin, and Achim Rosch for discussions. A.M.R. and K.H. are supported by grants from the NSF (PFC and PIF-0904017), the AFOSR, and a grant from the ARO with funding from the DARPA-OLE. M.H. is supported by DOE Grant No. de-sc0003910, and V.G. is supported by NSF Grants No. DMR-0449521 and No. PIF-0904017. K.H. thanks the Aspen Center for Physics, which is supported by an NSF grant, for its hospitality during the writing of this paper.

-
- [1] Y. Takasu *et al.*, *Phys. Rev. Lett.* **91**, 040404 (2003); T. Fukuhara, S. Sugawa, Y. Takasu, and Y. Takahashi, *Phys. Rev. A* **79**, 021601 (2009); T. Fukuhara, S. Sugawa, and Y. Takahashi, *ibid.* **76**, 051604 (2007); T. Fukuhara, S. Sugawa, M. Sugimoto, S. Taie, and Y. Takahashi, *ibid.* **79**, 041604 (2009); S. Kraft, F. Vogt, O. Appel, F. Riehle, and U. Sterr, *Phys. Rev. Lett.* **103**, 130401 (2009); S. Stellmer, M. K. Tey, B. Huang, R. Grimm, and F. Schreck, *ibid.* **103**, 200401 (2009); Y. N. Martinez de Escobar, P. G. Mickelson, M. Yan, B. J. De Salvo, S. B. Nagel, and T. C. Killian, *ibid.* **103**, 200402 (2009); P. G. Mickelson, Y. N. Martinez de Escobar, M. Yan, B. J. DeSalvo, and T. C. Killian, *Phys. Rev. A* **81**, 051601 (2010); *Phys. Rev. Lett.* **105**, 030402 (2010); M. K. Tey, S. Stellmer, R. Grimm, and F. Schreck, *Phys. Rev. A* **82**, 011608 (2010).
- [2] D. Hayes, P. S. Julienne, and I. H. Deutsch, *Phys. Rev. Lett.* **98**, 070501 (2007); A. J. Daley, M. M. Boyd, J. Ye, and P. Zoller, *ibid.* **101**, 170504 (2008); A. V. Gorshkov *et al.*, *ibid.* **102**, 110503 (2009); I. Reichenbach, P. S. Julienne, and I. H. Deutsch, *Phys. Rev. A* **80**, 020701 (2009); R. Stock, N. S. Babcock, M. G. Raizen, and B. C. Sanders, *ibid.* **78**, 022301 (2008); A. J. Daley, *Quantum Inf. Process.* **10**, 865 (2011).
- [3] A. V. Gorshkov *et al.*, *Nat. Phys.* **6**, 289 (2010).
- [4] T. Ido and H. Katori, *Phys. Rev. Lett.* **91**, 053001 (2003); A. D. Ludlow *et al.*, *Science* **319**, 1805 (2008); P. Lemonde, *Eur. Phys. J. Spec. Top.* **172**, 16 (2009); N. D. Lemke *et al.*, *Phys. Rev. Lett.* **103**, 063001 (2009); T. Hong *et al.*, *Opt. Lett.* **30**, 2644 (2005); T. Kohno *et al.*, *Appl. Phys. Express* **2**, 072501 (2009); A. Derevianko and H. Katori, *Rev. Mod. Phys.* **83**, 331 (2011).
- [5] S. Kotochigova, T. Zelevinsky, and J. Ye, *Phys. Rev. A* **79**, 012504 (2009).
- [6] K. Heyde, *Basic Ideas and Concepts in Nuclear Physics* (Institute of Physics, Bristol, UK, 1994).
- [7] Sugawa *et al.*, *Nat. Phys.* **7**, 642 (2011).
- [8] M. A. Cazalilla, A. F. Ho, and M. Ueda, *New J. Phys.* **11**, 103033 (2009).
- [9] M. Hermele, V. Gurarie, and A. M. Rey, *Phys. Rev. Lett.* **103**, 135301 (2009); N. Read and S. Sachdev, *ibid.* **62**, 1694 (1989); T. A. Toth, A. M. Laeuchli, F. Mila, and K. Penc, *ibid.* **105**, 265301 (2010); I. Affleck and J. B. Marston, *Phys. Rev. B* **37**, 3774 (1988); C. Honerkamp and W. Hofstetter, *Phys. Rev. Lett.* **92**, 170403 (2004).
- [10] F. F. Assaad, *Phys. Rev. B* **71**, 075103 (2005).
- [11] F. Werner, O. Parcollet, A. Georges, and S. R. Hassan, *Phys. Rev. Lett.* **95**, 056401 (2005).
- [12] R. Joerdens *et al.*, *Nature (London)* **455**, 204 (2008); U. Schneider *et al.*, *Science* **322**, 1520 (2008).
- [13] J. Oitmaa, C. Hamer, and W. Zheng, *Series Expansion Methods for Strongly Interacting Lattice Models*, reissue ed. (Cambridge University Press, Cambridge, UK, 2010).

- [14] R. Jördens *et al.*, *Phys. Rev. Lett.* **104**, 180401 (2010).
- [15] C. J. Pethick and H. Smith, *Bose-Einstein Condensation in Dilute Gases* (Cambridge University Press, Cambridge UK, 2001).
- [16] A. M. Rey, G. Pupillo, and J. V. Porto, *Phys. Rev. A* **73**, 023608 (2006).
- [17] T. Esslinger, *Annu. Rev. Condens. Matter Phys.* **1**, 129 (2010).
- [18] N. Gemelke, X. Zhang, C. Hung, and C. Chin, *Nature (London)* **460**, 995 (2009); W. S. Bakr *et al.*, *Science* **329**, 547 (2010); J. F. Sherson *et al.*, *Nature (London)* **467**, 68 (2010).
- [19] See Supplemental Material at <http://link.aps.org/supplemental/10.1103/PhysRevA.85.041604> for a discussion of the N-dependence of adiabatic loading at high temperatures, the weakly interacting gas scaling, and simple analytic limits of adiabatic loading.
- [20] W. Zwerger, *J. Opt. B* **5**, S9 (2003).
- [21] S. Taie *et al.*, *Phys. Rev. Lett.* **105**, 190401 (2010).
- [22] S. Fuchs *et al.*, *Phys. Rev. Lett.* **106**, 030401 (2011).
- [23] L. De Leo, C. Kollath, A. Georges, M. Ferrero, and O. Parcollet, *Phys. Rev. Lett.* **101**, 210403 (2008).
- [24] B. D. Esry, C. H. Greene, and J. P. Burke, *Phys. Rev. Lett.* **83**, 1751 (1999).

Supplementary information for: High temperature properties of fermionic alkaline earth atoms in optical lattices

Kaden R. A. Hazzard^{1,2,3}, Victor Gurarie², Michael Hermele², and Ana Maria Rey^{1,2,3}

¹ *JILA, University of Colorado, Boulder, Colorado 80309-0440, USA*

² *Department of Physics, University of Colorado, Boulder, Colorado 80309-0440, USA and*

³ *NIST, Boulder, Colorado 80309-0440, USA*

WHY, AT HIGH TEMPERATURES, HEATS RATHER THAN COOLS WITH INCREASING N

Figure 2 of the main text shows that at low temperature, increasing N for experimentally relevant N while fixing the initial temperature generates colder clouds. However, it also shows that the trend is reversed at higher temperatures. This may be somewhat counterintuitive, as at very high temperatures the entropy should become very high even in the deep lattice.

To understand this behavior, we first note that at the higher temperatures the density profiles are quite different than at low temperatures: they have lower central density and are more spread out. Fig. 1 illustrates this effect. In particular, there is no central Mott regime in the final states and it turns out this reduces the entropy's dependence on N . In particular, we recall that at low temperatures, the final state entropy grows with $\log N$, while the initial state grew with $N^{1/3}$ in three dimensions; for the $N \lesssim 20$ of interest, the former grew faster than the latter, leading to the cooling. In contrast, Fig. 1 illustrates that with the lower density clouds produced at high temperature, there is no Mott region and the entropy always scales roughly as $N^{1/3}$ rather than $\log N$, eliminating the cooling effect seen at low temperatures. The details of this heating will depend on the central filling, and will presumably usually occur at higher temperatures for higher central fillings.

We note that this behavior also follows directly in the $t \ll T \ll U$, central unit filling limit considered below.

WEAKLY INTERACTING GAS'S ENTROPY DEPENDENCE ON N AT FIXED PARTICLE NUMBER

In the main text we gave formulas for the particle number \mathcal{N} and entropy S of the weakly interacting trapped gas with the structure $\mathcal{N} \propto N(\mu/\omega)^d$ and $S \propto (T/\omega)N(\mu/\omega)^{d-1}$. Eliminating μ/ω in favor of \mathcal{N} in the entropy, we find $S \propto (T/\omega)N \left(\frac{\mathcal{N}}{N}\right)^{1-1/d} = (T/\omega)N^{1/d}\mathcal{N}^{1-1/d}$. In particular, this shows that in $d = 3$, $S \propto N^{1/3}$, a fact crucial in the text for our qualitative explanation of why, at low temperatures, increasing N leads to a temperature decreasing with N after adiabatically loading.

We also give a geometric picture to understand this

dependence. Fixing the number of particles fixes the Fermi surface volume to some value V . If there are N flavors of fermions, this volume is distributed over N equal Fermi spheres of volume V/N . At low temperatures, the entropy is proportional to the Fermi surface area times the temperature. The Fermi surface area is N times the Fermi surface area of each Fermi sphere, namely $N(V/N)^{(d-1)/d} = V^{1-1/d}N^{1/d}$. Since the entropy is proportional to this, this gives the scaling $N^{1/d}$ derived above.

SCALING IN $t \ll T \ll U$ LIMIT WITH UNIT CENTRAL FILLING AND CENTRAL μ LOW TO NEGLECT MULTIPLE OCCUPANCIES

For general parameters, the adiabatic loading calculation of the main text admits no analytic solution. However, under certain conditions (detailed below) an analytic solution is possible. We expect this simple limit to provide a useful approximation and framework in which to interpret the numerical results.

Specifically, we can analytically calculate the results in the following conditions: (1) we use the zero'th order high-temperature expansion applies, (2) $t \ll T \ll U$ (this augments the usual criterion for the high-temperature series, $t \ll T$), (3) central filling equal to one (equivalent to a condition on the central chemical potential), and (4) the central chemical potential small enough that multiple occupancies are negligible. We comment on the validity of these conditions. The approximation in (1) is accurate at high temperatures $T \gtrsim t$, as argued on general grounds in the text and demonstrated for one case in Fig. 2. Condition (2) is the most important regime considered in the paper, as it is deep in the Mott state and the aim of current experiments. It is also the regime in which the decrease of final temperature with increasing N takes place. Condition (3) and (4) are satisfied in many experiments and correspondingly are satisfied for the experimentally realistic parameters we used to generate Fig. 2. Thus, note that these conditions are experimentally relevant and encompass the most important region of the results shown in Fig. 2 of the main text.

Under conditions (1), (3), and (4) above, we can neglect multiple occupancies and the partition function of the homogeneous system simplifies to $z_0 \approx 1 + Ne^{\beta\mu}$, and the density and entropy may be obtained from this

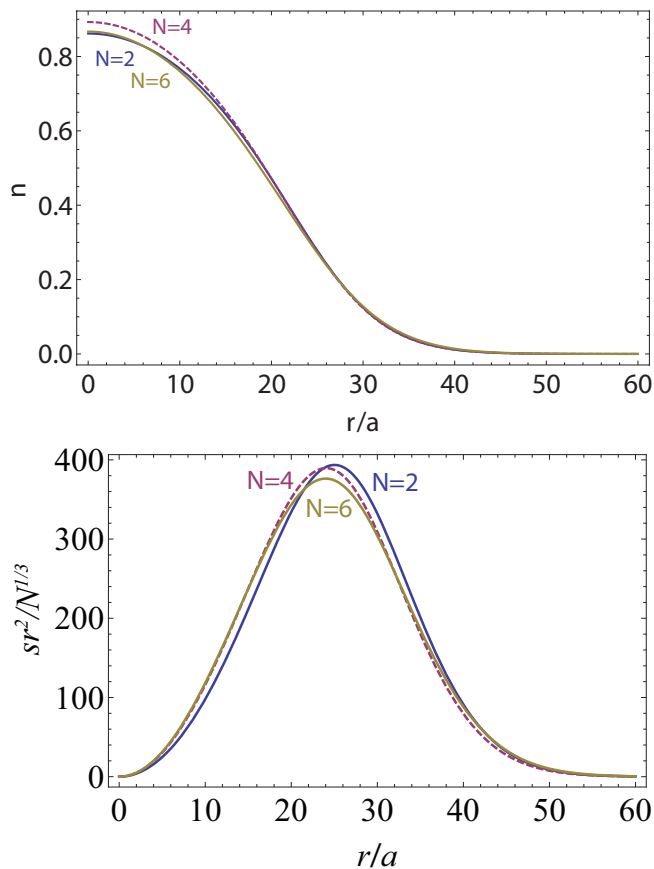


FIG. 1: Top: density profiles for $N = 2, 4, 6$ (bottom curves are $N = 2$ and $N = 6$, colored blue and gold, respectively, and are extremely similar; top curve is $N = 4$.) of final states after adiabatic loading for $T_i/\omega = 14.7$ and other parameters corresponding to Fig. 2 of the main text. Note the absence of a Mott regime at these high final temperatures. Bottom: entropy profiles for $N = 2, 4, 6$ (top/blue, middle/dashed/purple, bottom/gold respectively), rescaled by $r^2/N^{1/3}$, of final states after adiabatic loading for $T_i/\omega = 14.7$ showing that the entropy scales as $N^{1/3}$ at these high temperatures rather than the more favorable $\log N$ obtained at lower temperatures. (The r^2 is the surface area factor that multiplies the entropy density in the integral to obtain the total entropy, and is included simply so one may more easily see what regions of the system contribute most to the total entropy.)

by taking derivatives as discussed in the main text. To obtain the final temperatures under the assumption of adiabaticity, we must calculate the total particle number \mathcal{N} and entropy S of the trapped system as a function of temperature and find the temperature that matches these to the initial conditions. In the LDA, the \mathcal{N} and S are then polylogarithms. Conditions (2) and (3) allow us to asymptotically expand these for $\beta\mu_c \gg 1$ where μ_c is the central chemical potential (these are generalizations of

the usual Sommerfeld expansion). Then one finds for the trapped lattice system $S = \mathcal{N} \log N + \frac{\pi T}{8} (3A^2\mathcal{N}/2)^{1/3} + T$ (nK)

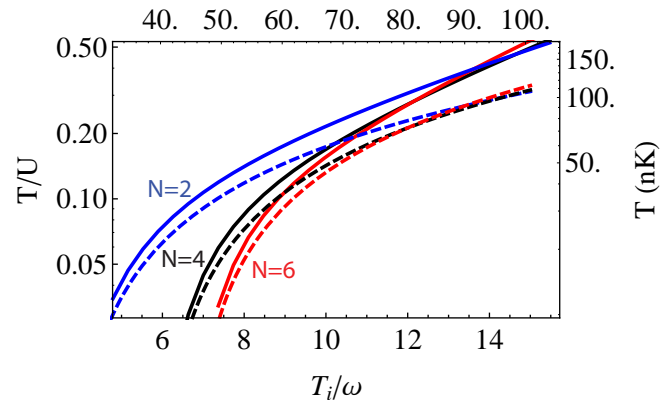


FIG. 2: Final temperature T/U after adiabatically loading a weakly interacting trapped gas at temperature T_i/ω for $N = 2, 4, 6$ in the atomic limit $t/U = 0$ (solid line) and in the no-multiple-occupancy, $t \ll T \ll U$ limit specified in this section (dashed line). The parameters are the same as for Fig. 2 of the main text.

$O(T^2)$. Matching S and \mathcal{N} to the initial entropy and particle number of the weakly interacting gas (with formulas given in the main text) yields the final temperature T_f in terms of the initial gas temperature T_i . We find

$$T_f \approx aN^{2/3} \frac{T_i}{\omega} - b \log N \quad (1)$$

with

$$a = XN^{1/3}\pi^2 \quad (2)$$

and

$$b = X6^{1/3}N^{2/3}, \quad (3)$$

where $X = \frac{6^{1/3}ma^2\omega^2}{\pi^{5/3}(5\pi-1)}$.

Fig. 2 compares the results of the calculation in this limit of the high-temperature expansion with the full high-temperature expansion shown in the text. For temperatures $T/U \lesssim 0.1$, the approximation is quite good in this situation, and it captures the qualitative physics to temperatures of $T/U \approx 0.2$ or higher.

This approach captures, for small T_i/ω , the decreasing of T_f with increasing N : here the second term dominates and the horizontal intercept of the T_f curve decreases due to the $\log N$ factor. It also explains the reversal of this trend at higher temperatures discussed previously in the Supplementary Information: here the first term dominates and T_f increases as $N^{2/3}$.